



# Segmentation Using Adaptive Fuzzy Clustering Based Atom Search Optimization of Magnetic Resonance Images for Early Detection of Alzheimer's Disease

Nirupama P. Ansingkar<sup>1</sup>(✉), Rita B. Patil<sup>1</sup>, Rajmohan A. Pardeshi<sup>1</sup>,  
and Prapti D. Deshmukh<sup>2</sup>

<sup>1</sup> Dr. Babasaheb Ambedkar Marathwada University, Aurangabad, India  
[nirupatodkar@gmail.com](mailto:nirupatodkar@gmail.com)

<sup>2</sup> MGM, Dr. G. Y. Pathrikar College of CS and IT, Aurangabad, India

**Abstract.** Alzheimer's Disease is a neurodegenerative condition affecting middle-aged to older people characterized by marked loss of memory, cerebral damage and helplessness. Early and correct detection can help doctors to plan the medication for the sufferer. As we know this disease is progressive and degenerative, the speed of the disease can slow down by appropriate treatment it also helps to protect against brain tissue damage. This work presents the practical methodology, pre-processing and segmentation steps which helps in the early detection of Alzheimer's disease. The effective pre-processing of an image is done with the help of skull stripping as the first step, then normalized linear smoothing and median joint(NLSMJ) Filtering and segmentation is carried out with Adaptive Fuzzy Based Atom Searched Optimization. The presented technique is used on Local neuro-imaging MRI dataset collected from MGM hospital.

**Keywords:** Alzheimer's disease · pre-processing · DT · NLMSMJ · MGM dataset · MRI

## 1 Introduction

Dementia is an irreversible deterioration of the mental state of an individual. The problems like cognitive thinking, memory loss, cerebral damage, helplessness, change in personality and the person can face the problem in communication with others at home and social environment [1]. Illness is multiplied in the scope of 4–6 years [2, 3]. Alois Alzheimer described the disease for the first time. There is a pathological shrinking of the brain is done due to the loss of neurons and the neurons also lose the connection mainly in hippocampus. It shows the abnormal accumulation of tau protein in the brain causing disturbance in the

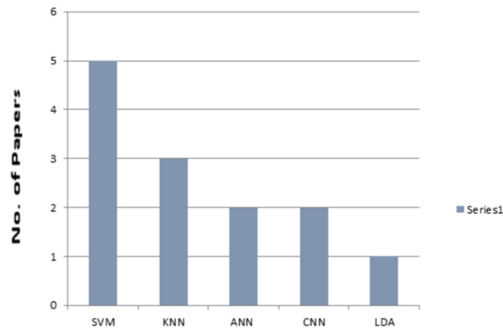
signal trans-mission and also shows the presence of amyloid plaques in hippocampus. In the last stage, neocortical areas are affected [4]. Three different stages are involved in the diagnosis of AD. Consultation with neural physician is necessary for the first stage. The second stage is to undergo various neuropsychological tests like COG, BoMC, MMSC, BDIMC, AD8, MOCA, and GP are used, and the third stage is taking MRI scans [5]. Various neuroimaging techniques are used for the detection of AD-like PET scan, CT-scan, MRI, structural MRI, and many more. AD can be easily detected by MRI which is the authentic and painless way. Histological changes like atrophy, amyloid plaques and hypo metabolism which are degenerating changes in the brain can be captured through medical imaging [6, 7]. Dementia is an umbrella under which many neural disorders are considered like Lewy body, Parkinson's disease, Alzheimer's disease and many neurodegenerative diseases [8–11]. Now a days, diagnosis of AD would be possible using various machine learning algorithms which leads to the proper identification of AD. In neurology and neuro-surgery, Magnetic Resonance Imaging (MRI) is the most commonly used test which provides the details of the vascular anatomy, brain, spinal cord in coronal, axial and sagittal planes. MRI is based on magnetization properties. It makes use of powerful magnets which produce a strong magnetic field that forces protons in the body to align with that field.

## 2 Related Work

SamanSarraaf et al. [13] had taken T1 weighted scans for the project. First ten images were excluded as they do not have any functional information. For pre-processing, skull stripping, motion correction and spatial smoothing had applied on the scans. The noise was removed using high-pass temporal filtering. The product of pre-processing step was  $45 \times 54 \times 45 \times 300$  images. Derby CA [14] pre-processing was done with the help of statistical software SPM2. A customized template was constructed to the standard MNITI. Low dimensional transformation algorithm was implemented in SPM2 Ruiz E, Ramirez Jet al. [15] all DICOM scans were converted into NIFTI format. Pre-processing was done using FSL software to get normalized MD and FA volume. In the next stage skull stripped template was created and non-linear affine registration was done. Chyzyhyk D et al. [16] VBM was computed SPM, spatial mask was used for feature extraction. The image was pre-processed using following steps were segmentation, Gaussian smoothing using FWHM and thresholding. Yue L, Gong Xet al. [17] The structural MRI scans were obtained from 3.0 T SIEMENS scanners. Pre-processing was done with N3 algorithm 1.

**Table 1.** Table of Literature Review

	Author	Database Used	Pre-processing	Classification	Groups
A Novel Method for the Classification of Alzheimer's Disease from Normal Controls using Magnetic Resonance Imaging	Riyaj Uddin Khan et al.	ADNI T1 weighted MRI scan	Free-Surfer S/W package V6.0	Twin SVM (TSVM), least square TSVM (LST SVM), robust energy based least square twin SVM(RELS-TSVM)	Normal Con-trol(NC), Mild Cognitive Im-pairment (MCI) and Alzheimer's Disease(AD)
A Multi-modal Deep Convolutional Neural Net-work for Automatic Hippocampus Segmentation and Classification in Alzheimer's Disease	Man-hua Liu et. al.	ADNI T1 weighted Structural MRI scan	Resize, skull strip-ping, cere-bellum removal, intensity normalization	Multi-task CNN and Dense-Net Model	Normal Con-trol(NC), Mild Cognitive Impairment (MCI) and Alzheimer's Disease(AD)
Diagnosis of Alzheimer's Dis-ease Based on Structural MRI Images using a Regularized Extreme Learning Machine and PCA Features	Ramesh Kumar Lama et. al.	ADNI T1 weighted Structural MRI scan	Free-Surfer S/W package V5.0	Support Vector Machine (SVM), Import Vector Machine (IVM), Regularized Extreme Learning Machine(RELM)	Healthy Control(HC), Mild Cognitive Impairment (MCI) and Alzheimer's Disease(AD)
Automatic Machine Learning Classification of Alzheimer's Disease based on Selected Slices from 3D Magnetic Resonance Imaging	Abdalla R. Gad et. al.	National Alzheimer's Coordinating Centre(NACC) 3D T1 weighted MRI	Noise removal, normalization using ROI	K- Nearest Neighbor(KNN), Support Vector Machine (SVM)	Normal Control(NC), Mild Cognitive Impairment (MCI) and Alzheimer's Disease(AD)
Alz-heimer's disease: 3- Dimensional MRI texture for prediction of conversion from mild cognitive impairment	Collin C. Luk et. al.	ADNI T1 weighted MRI scan	ROI is used for segmenta-tion	ANN( Artificial Neural Network) K- Near-est Neigh-bor(KNN), Support Vector Machine (SVM)	Normal Control(NC), Mild Cognitive Im-pairment (MCI) and Alzheimer's Disease(AD)
Early diag-nosis of Alzheimer's Disease Based on Resting- State Brain Net-works and Deep Learning	Rong-hui Ju et. al.	ADNI R-fMRI	Motion Correction, Slice timing correction, skull stripping, normalization, smoothing and ROI	LDA, LR, SVM, and the auto encoder network	Normal Control(NC), Mild Cognitive Impairment (MCI) and Alzheimer's Disease(AD)
Multi-Modal Neuroimaging Feature Learning for Multi-Class Diagnosis of Alzheimer's Disease	Siqi Liu, Si-dong Liu et al.	ADNI T1 weighted MRI scan and FDGPET images	Noise removal and extraction of ROI	SVM and SAE	Normal Control(NC), Mild Cognitive Impairment (MCI) and Alzheimer's Disease(AD)

**Fig. 1.** Analysis of Classification Techniques Used for Detection of Alzheimer's Disease

### 3 Methodology

This paper presents preprocessing and segmentation technique which leads to the detection of Alzheimer's Disease. Figure 2. Shows the workflow diagram. Back-ground is excluded with the double threshold (DT) based skull stripping.

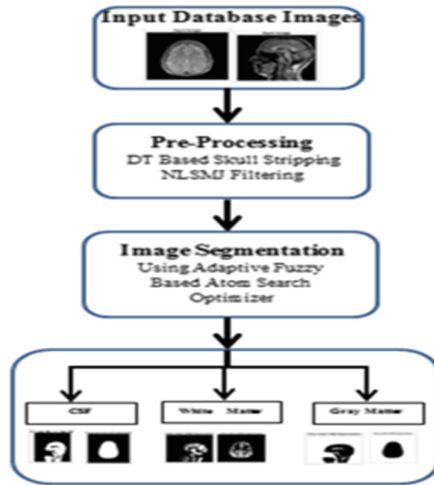


**Fig. 2.** Block Diagram of the Steps involved in Segmentation of the MRI Image into Cerebrospinal Fluid, White Matter and Gray Matter

After the application of DT, Normalized Linear Smoothing Median Joint filtering is used for noise removal. Doing above steps, preprocessing is done. Segmentation is done on the preprocessed image. In segmentation we separated three regions, first region is grey matter(GM), second region is white matter(WM), and the third region is cerebrospinal fluid(CFS) are segmented by using fuzzy based atom search optimizer. Segmentation accuracy is obtain by the optimizer because it has a high convergence rate for enhancement of segmentation [14].

### 3.1 Image Pre-processing

Initially, skull stripping is done with the help of double thresholding, then with Normalized Soothing and Median Joint filtering, the image is enhanced. Pre-processing procedure is explained below.

**3.1.1 DT-Based Skull Stripping.** Skull is stripped using double thresholding. Intensity differentiation of skull is done in two ranges as 0 to 0.5 and 0.7 to 1. High intensity range is skull region which is brighter than the other region and is removed from the image. Skull stripping is done as shown in equation (1).

$$I(a, b) = \begin{cases} 1 & \text{for } 0.2 \leq D_r \leq 0.7 \\ 0 & \text{else} \end{cases} \quad (1)$$

Here, represents the skull stripped image and represents the double threshold. Here, the skull region is above 0.7 range.

**3.1.2 Normalized Linear Smoothing and Median Joint (NLSMJ) Filtering.** Images which are acquired at different condition must have same characteristics. For that minimum and maximum normalization is applied, through this we can fit image in fixed dimension. The condition is given in equation (2)

$$\bar{N}_J(Z) = \frac{X - X_{min}}{X_{max} - X_{min}} \quad (2)$$

Here,  $\bar{N}_J$  is the normalized image for input image  $X$ ,  $X_{min}$  and  $X_{max}$  are the minimum and maximum values in image  $X$ . Variation in range of the intensity values is reduced by normalization process. The intensity deviation is decreased using linear smoothing filtering. Pixel value of each pixel is replaced by taking the average of its neighborhood pixels. It removes the dissimilar pixel nearby. The linear smoothing filtering is described by equation(3),

$$\bar{F}(x, y) = \frac{1}{cd} \sum_{(u,v) \in R_{y,z}} g(w, z) \quad (3)$$

The set of coordinates is denoted by  $R_{y,z}$  in the rectangular sub image window, the middle pixels is denoted by  $(x,y)$  and the noisy image is represented as  $g(w,z)$ . The image is enhanced by combining filtering with median filter. Intensity variation is improved with linear smoothing filter. Edge details are restored with median filter. Jointly it enhances the quality of the image which is shown in equation (4)

$$\bar{F}(x, y) = Md_{(s,t) \in K_{yz}} \{g(j, k)\} \quad (4)$$

Here,  $K_{yz}$  represents the set of coordinates at a point centered  $(x,y)$ . filtering removes the noise in the digital image. Noise decreases the quality of an image. To remove noise, the filtering process is used.

### 3.2 Image Segmentation Using Adaptive Fuzzy Clustering Based Atom Search Optimization

After pre-processing, the image is clustered. The image is clustered into CSF, white matter and gray matter. Centroid sets are generated as mention in the equation (5)

$$S^{(0)} = \{S_1^{(0)}, S_2^{(0)}, S_3^{(0)}, \dots, S_k^{(0)}\} \quad (5)$$

The membership function matrix  $M^{(f)} = \{m_{st}^{(f)}\}$  is attained through the individual membership functions through the subsequent condition (6),

$$m_{st}^{(f)} = \frac{1}{\sum_{f=1}^k \left( \frac{\|Y_s - q_t^{(f)}\|}{\|Y_s - q_k^{(f)}\|} \right)^{2/(k-1)}} \quad (6)$$

Here,  $||.||$  represents the Euclidean distance between the centre and perceived data,  $k$  represents the index of the fuzziness coefficient range from 1 to infinity. The centroid  $C_k^{(p+1)}$  at  $(p+1)^{th}$  step is updated through the equation (7),

$$C_t^{(p+1)} = \frac{\sum_{s=1}^n m_{st}^{(p+1)k} Y_t}{\sum_{s=1}^n m_{st}^{(p+1)k}} \quad (7)$$

through the atom search optimization procedure, centroid position is updated. Clustering pixels location is updated through the equation (8),

$$Z_k(t' + 1) = Z_k(t') + \bar{V}_k(t' + 1) \quad (8)$$

Here,  $_k(t')$  represents the location of the  $k^{th}$  pixel in the  $t^{th}$  iteration  $Z_k(t' + 1)$  represents the location of  $k^{th}$  pixel in the  $(t + 1)^{th}$  iteration and  $\bar{V}_k(t' + 1)$  represents the velocity of the  $k^{th}$  atom in the  $(t + 1)^{th}$  iteration and it is evaluated through the condition (9) as,

$$\bar{V}_k(t' + 1) = \hat{J}(C, M) * \bar{V}_k(t') + a_k(t') \quad (9)$$

Here,  $\hat{J}(C, M)$  signifies the initially attained clustering outcomes and  $a_k(t')$  represents the acceleration of the  $k^{th}$  atom in the  $t^{th}$  iteration and it is attained through the condition (10),

$$\begin{aligned} a_k(t') = & -\bar{\eta}(t') \sum_{k \in N_{best}} \frac{\hat{R} \left[ 2 * (q_{pk}(t'))^{13} - (q_{pk}(t'))^7 \right]}{D_p(t')} \times \frac{Z_p(t') - Z_k(t')}{Z_p(t') * Z_k(t')} \\ & + \hat{\beta} e^{\frac{-20I_{max}}{I_{max}}} \frac{Z_{best}(t') - Z_p(t')}{D_p(t')} \end{aligned} \quad (10)$$

Here,  $N_{best}$  represents the best atoms set,  $Z_{best}$  represents the best atom in the current location,  $\hat{\beta}$  represents the weights of the multiplier and  $\bar{\eta}(t')$ ,  $q_{pk}(t')$ ,  $D_p(t')$  functions are evaluated with the subsequent conditions are described as,

$$\bar{\eta}(t') = \alpha_w \left( 1 - \frac{1 - 1}{I_{max}} \right) * e^{\frac{-20I_{max}}{I_{max}}} \quad (11)$$

$$q_{pk}(t') = \begin{cases} q_{min}, & \frac{d_{pk}(t')}{\sigma(t')} < q_{min} \\ \frac{d_{pk}(t')}{\sigma(t')}, & q_{min} \leq \frac{d_{pk}(t')}{\sigma(t')} \leq q_{max} \\ q_{max}, & \frac{d_{pk}(t')}{\sigma(t')} > q_{max} \end{cases} \quad (12)$$

$$d_p(t') = \frac{D_p(t')}{\sum_{k=1}^{\bar{N}} D_k(t')} \quad (13)$$

Here,  $\alpha_w$  denotes the depth weight,  $I_{max}$  represents the maximum number of iterations and  $d_{pk}(t')$  represents the distance among  $p^{th}$  and  $k^{th}$  atoms at the

$t^{th}$  iteration. Moreover, the variables  $q_{min}, q_{max}$ ,  $\sigma(t')$  and  $D_p(t')$  are evaluated through the subsequent equation (14),

$$q_{min} = \bar{g}_0 + \bar{g}(t') \quad \& \quad q_{max} = \bar{u} \quad (14)$$

$$\sigma(t') = Z_{pk}(t'), \frac{\sum_{k \in N_{best}} Z_{pk}(t')}{k(I_{max})} \quad (15)$$

Errors are reduced through the clustering iterations through condition (16),

$$\hat{J}(C, M) = \sum_{S=1}^n \sum_{t=1}^k m_{st}^k ||Y_s - q_t||^2 \quad (16)$$

By using atom search optimization, the results are obtained. The accurate clustering of cerebrospinal fluid, white matter and grey matter is attained through condition (16). The final fitness is obtained through the condition (17),

$$D_p(t') = e^{-\frac{Fitness_k(t) - Fitness_{best}(t)}{Fitness_{worst}(t) - Fitness_{best}(t)}} \quad (17)$$

The process is repeated until the maximum iteration reaching the satisfying solution with the condition of  $||D_p^{k+1}(t') - D_p^k(t')|| < \epsilon$ . The proposed clustering method efficiently segments the three regions of CSF, white matter and grey matter in the images.

## 4 Dataset Description: Local Dataset

Magnetic Resonance Images are collected from MGM hospital which is comprised of 750 scan images of people aged from 33 to 85. The database has cognitive normal (CN), Mild cognitive impairment (MCI), and Alzheimer's disease (AD) brain categories. MGM hospital is situated in Aurangabad City of Maharashtra State therefore the selected subjects were from Aurangabad district and marathwada region of Maharashtra state. Total 50 images are processed. The input images of type sagittal and axial type of the MGM Hospital database is used for segmentation. Initially, input sample sagittal skull images are considered. Three different input images of different patient are taken as an input sample images of the MGM database is represented in Fig. 3, the outcome of skull-stripped images are shown in Fig. 4, the outcome of filtered images is shown in Fig. 5, and segmented Cerebrospinal Fluid, White Matter and Gray Matter regions are shown in Fig. 6.

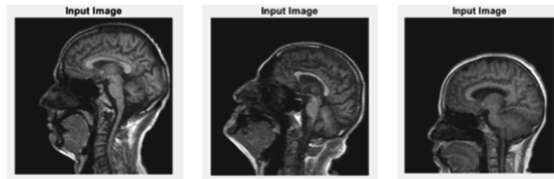


**Fig. 3.** Sample input images of MGM Hospital database



Fig. 4. Outcome of skull-stripped images



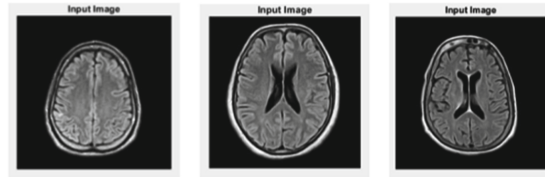
Fig. 5. Outcome of filtered images



Fig. 6. Outcome of segmented CSF, White matter and Grey matter regions



Another set of axial type MRI sample images taken from the MGM hospital dataset with a skull region is represented below. The input sample images of the MGM dataset with skull region are shown in the Fig. 7. The output of skull stripped images is shown in Fig. 8. The outcome of filtered images is shown in Fig. 9 and segmented CSF, WM and GM regions are shown in Fig. 10.



**Fig. 7.** Sample input images of MGM Hospital dataset

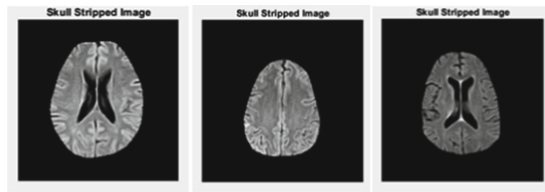


**Fig. 8.** Skull Stripped images of MGM Hospital dataset

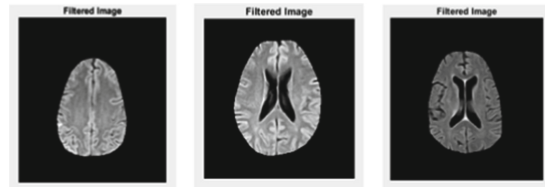


**Fig. 9.** Outcome of filtered input images

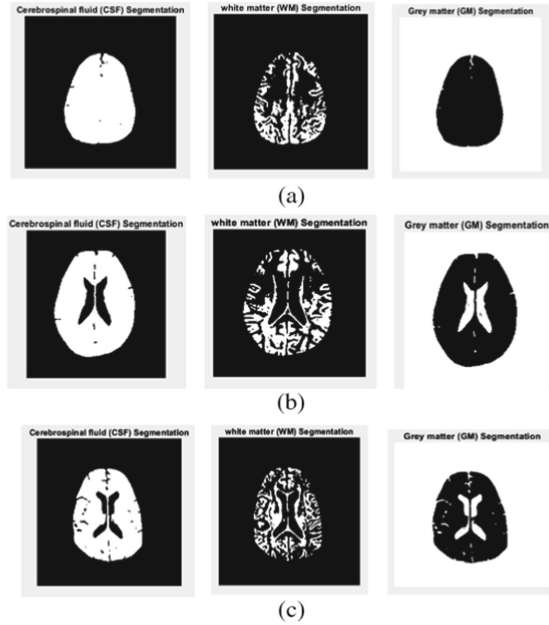


**Fig. 10.** Outcome of segmented CSF, White matter and Grey matter

## 5 Conclusion

The paper presents the outcome of segmentation which is the first step towards the diagnosis of Alzheimer's disease and plays an important role in finding out the proper stage or progress of the disease. The appropriate steps for pre-processing lead to the proper segmentation. An input image is pre-processed using double thresholding is used for skull stripping to differentiate the intensities leads the image and Normalized Linear Smoothing Median Joint filter (NLSMJ) is used for image enhancement. Adaptive fuzzy-based atom search optimization is applied on the filtered image to segment the image into CSF, GM, and WM. The proper segmentation helps in finding out the proper stage of Alzheimer's disease after extracting the proper features.

## References

1. ChuanChuan Zheng, Yong Xia, YongshengPan(2016)Automated identification of de-mentia usingmedical imaging: a survey from a pattern classification perspective. *Brain Informatics*(2016) 3:17-27,DOI 10.1007/s40708-015-0027-X
2. Abdalla R. Gad, N. M. Hussein Hassan, Rania A. AbulSeoud, Tamer M. Nassef, Automatic Machine Learning Classification of Alzheimer's Disease Based on selected Slices from 3D Magnetic Resonance Imaging, *International Journal of Biomedical Science and Engineering* ISSN:2376-7227(print) (2016).

3. Rakesh Kumar Lamba, JeonghwanGwak, Jeong-Seon Park and Sang-Woong Lee, Diagnosis of Alzheimer's Disease Based on Structural MRI Images Using a Regularized Extreme Learning Machine and PCA Features, Hindawi, Journal of Health-Care Engineering, Article ID 5485080, 11pages(2017).
4. S. R. Bhagyashree et al., "An Initial Investigation in the Diagnosis of Alzheimer's Disease using Various Classification Techniques." 978-1-4799-3975-6/14 IEEE (2014).
5. Thies W, Bleiler L (2013) "Alzheimer's Facts and Figures, Alzheimer's Dement(Journal ofAlzheimer'sAssociation),ElsevierInc.Mar(2013)
6. ChuanChuan Zheng et al., "Automated Identification of Dementia Using Medical Imag-ing: ASurvey from Pattern Classification Perspective," Brain informatics, 3:17-27 DOI 10.1007/s40708-05-0027Springer (2016).
7. Gomez Isla T et al. "Profound loss of layer II entorhinal cortex neurons occurs in very mild Alzheimer's disease." J. Neurosci 16(14):4491-4500(1996)
8. Chan D et al. "Rates of global and regional cerebral atrophy in AD and front o temporal dementia." Neurology57(10):1756-1763(2001)
9. Fox NC, Schott JM Imaging cerebral atrophy: normal aging to Alzheimer's Disease. TheLancet363(9406):392-394 (2004)
10. Resnick SM et al. "Longitudinal magnetic resonance imaging studies of older adults: ashinking brain." J. Neurosci. 23(8):3295-3301(2003)
11. Grossman M et al. "What's in a name: voxel-based morphometric analyses of MRI and naming difficulty in Alzheimer's Disease, fronto temporal dementia, and corticobasal degeneration" Brain 127 (Pt3):628-649 (2004).
12. Siq. Liu, Sidong Liu et al. "Multimodal Neuroimaging Feature Learning for Multi-class Diagnosis of Alzheimer's Disease" , IEEE Trans. Biomed Eng. : 62x(4) : 1132-1140, boi: ten1109/TBME2014.2372011 april (2015).
13. Sarraf S and Tofighi G Classification of Alzheimer's disease using fMRI data and deep learning convolutional neural networks."arXiv preprint arXiv : 1603.08631 (2016)
14. N. P. Ansingkar, Rita. B. Patil , P. D. Deshmukh, "An efficient multi-class Alzheimer detection using hybrid equilibrium optimizer with capsule autoencoder," Multimedia Tools and Applications, <https://doi.org/10.1007/s11042-021-11786-z>, Springer(2019).
15. DerbyCA et. al. "Trends in the public health significance, definitions of disease, and implications for prevention of Alzheimer's disease." Current Epidemiology Reports 7(2):68-76(2020)
16. Ruiz E, Ramirez J, Górriz JM, Casillas J "Alzheimer's disease computer-aided diagnosis: histogram-based analysis of regional MRI volumes for feature selection and classification." Journal of Alzheimer's disease 65(3):819-842(2018)
17. Chyzyk D, Savio A and Graña M Evolutionary ELM wrapper feature selection for Alzheimer's disease CAD on anatomical brain MRI. Neurocomputing 128:73-80 (2014).
18. YueL, GongX, ChenK, MaoM, LiJ, Nandi A KandLiM Autodetection of Alzheimer's Disease Using Deep Convolutional Neural Networks .In 2018 14th International Conference on Natural Computation, Fuzzy Systems and Knowledge Discovery (ICNC-FSKD),IEEE,228-234(2018)
19. Riyaj Uddin Khan et al. A Novel Method for the Classification of Alzheimer's Disease from Normal Controls using Magnetic Resonance Imaging, Experts systems, WILEY <https://doi.org/10.1111/exsy.12566>(2021-22)

20. Manhua Liu, Fan Li, Hao Yan et al. A Multimodal Deep Convolutional Neural Network for Automatic Hippocampus Segmentation and Classification in Alzheimer's Disease, *NeuroImage* <https://doi.org/10.1016/j.neuroimage.2019.116459> published by Elsevier Inc(2019).
21. Ramesh Kumar Lama, Jeonghwan Gwak et. al. Diagnosis of Alzheimer's Disease Based on Structural MRI Images using a Regularized Extreme Learning Machine and PCA Features, *Hindawi, Journal of Healthcare Engineering*, Volume 2017, Article ID 5485080, 11 pages, Hindawi <https://doi.org/10.1155/2017/5485080> (2017)
22. Abdalla R. Gad, N. M. Hussein et. al. Automatic Machine Learning Classification of Alzheimer's Disease based on Selected Slices from 3D Magnetic Resonance Imaging, *International Journal of Biomedical Science and Engineering*; 4(6):50-54, <http://www.sciencepublishinggroup.com/j/ijbse>, <https://doi.org/10.11648/j/ijbse.20160406.11> ISSN: 2376-7227(Print); ISSN: 2376-7235(Online) (2016)
23. Collin C. Luk, Abdullah Ishaque et. al., Alzheimer's disease: 3-Dimensional MRI texture for prediction of conversion from mild cognitive impairment, *Alzheimer's and Dementia: Diagnosis, Assessment and Disease Monitoring* 10755-763 ELSEVIER. <https://doi.org/10.1016/j.dadm.2018.09.002> (2018)
24. Ronghui Ju et. al. Early diagnosis of Alzheimer's Disease Based on Resting- State Brain Networks and Deep Learning, *IEEE/ACM TRANSACTIONS ON COMPUTATIONAL BIOLOGY AND BIOINFORMATICS* 2017. <http://www.ieee.org> (2017)
25. Siqi Liu, Sidong Liu, Weidong Cai et al., Multi-Modal Neuroimaging Feature Learning for Multi-Class Diagnosis of Alzheimer's Disease, *IEEE Trans Biomed Eng.* 2015; 62(4):1132-1140. <https://doi.org/10.1109/TBME.2014.2372011> (2015).

**Open Access** This chapter is licensed under the terms of the Creative Commons Attribution-NonCommercial 4.0 International License (<http://creativecommons.org/licenses/by-nc/4.0/>), which permits any noncommercial use, sharing, adaptation, distribution and reproduction in any medium or format, as long as you give appropriate credit to the original author(s) and the source, provide a link to the Creative Commons license and indicate if changes were made.

The images or other third party material in this chapter are included in the chapter's Creative Commons license, unless indicated otherwise in a credit line to the material. If material is not included in the chapter's Creative Commons license and your intended use is not permitted by statutory regulation or exceeds the permitted use, you will need to obtain permission directly from the copyright holder.

